Dynamic Properties of Supercritical C_{14}TEMPO Monolayers at the Air/Water Interface

Michael J. Johnson,[†] David J. Anvar,[†] Janusz J. Skolimowski,[‡] and Marcin Majda*[,†]

Department of Chemistry, University of California at Berkeley, Berkeley, California 94720-1460, and Department of Organic Chemistry, University of Łódź, Narutowicza 68, 90-136 Łódź, Poland

Received: August 28, 2000; In Final Form: October 19, 2000

Monolayers of 4-tetradecaneamido-2,2,6,6-tetramethyl-1-piperidinyloxy (C_{14}TEMPO) were investigated at the air/water interface. Pressure−area diagrams and Brewster angle microscopy provided evidence of supercritical state of this monolayer at temperatures as low as 2 °C. The supercritical character of C_{14}TEMPO Langmuir monolayers allowed the 2-D voltammetric measurements of its lateral diffusion constant, *D*, to be extended into a previously inaccessible region of low surface densities with mean molecular areas $A \sim 600$ Å^2/molecule. At $A > 250$ Å^2/molecule, *D* becomes independent of the C_{14}TEMPO surface concentration and depends solely on the hydrodynamic coupling of the polar headgroup to the aqueous subphase. These measurements and the supercritical state of C_{14}TEMPO monolayer open a possibility to probe the viscoelastic properties of the water liquid−vapor interfacial region.

Introduction

Langmuir monolayers are quasi 2-D films of water-insoluble amphiphiles formed and investigated at the air/water interface.[1] Langmuir films of phospholipids have many properties mimicking biological membranes.[2] Not surprisingly, Langmuir monolayers have been the subject of intense investigations.[3−7] Their structure and phase behavior have been studied using X-ray diffraction techniques,[5,8] Brewster angle microscopy (BAM),[9,10] epifluorescence microscopy, and other methods.[3,4,7] These investigations concerned primarily the condensed phases of the phospholipid and long chain fatty acid monolayers. In comparison, the liquid expanded (LE) and gaseous (G) phases of Langmuir monolayers, as well as the related LE/G phase transition, are less well understood. Due to experimental difficulties, determination of the LE/G critical temperature ($T_c^{(l)}$) has been rather elusive and is known only for a few aliphatic acids and their derivatives. The $T_c^{(l)}$ values near or below room temperature were reported for lauric, tridecanoic, and myristic acids, for their ethyl esters, and for myristic nitrile by Adam and Jessop.[11] However, there is no agreement in the measurements of the $T_c^{(l)}$ value for pentadecanoic acid. While this amphiphile has been one of the most thoroughly investigated monolayer systems, the reported $T_c^{(l)}$ values range from 26 to 70 °C.[4,12,13]

Here, we report dynamic properties of Langmuir monolayers of an electrochemically active amphiphile, 4-tetradecaneamido-2,2,6,6-tetramethyl-1-piperidinyloxy (C_{14}TEMPO). Using classical Langmuir trough measurements, Brewster angle microscopy, and 2-D voltammetry,[14] we discovered that, at temperatures as low as 2 °C, C_{14}TEMPO Langmuir monolayers do not exhibit the liquid/gas (LE/G) phase transition upon their expansion. This room-temperature supercritical character of C_{14}TEMPO allowed us to investigate its lateral mobility on the water surface over a broad range of surface densities. This spans not only a liquid region, which for many Langmuir monolayers has been accessible by fluorescence recovery after photobleaching (FRAP)[15,16] and 2-D voltammetry, but also a previously inaccessible region of very high mean molecular areas (*A*), extending to ∼600 Å^2/molecules. We show that upon expansion, the lateral mobility of C_{14}TEMPO initially increases, reflecting a known decrease of monolayer viscosity. However, beyond ∼300 Å^2/molecule, a plateau develops in a plot of the lateral diffusion constant, *D* vs *A*. In that region, the lateral mobility is no longer affected by chain−chain interactions. Instead, it depends solely on the hydrodynamic coupling of the polar headgroups to the subphase. These measurements open, for the first time, a possibility to probe the viscoelastic properties of the water liquid−vapor interfacial region. The importance of the water liquid−vapor interface is difficult to overemphasize. Its properties[17−19] and the nature of monolayer phenomena associated with this interface govern the behavior of biological systems and are of fundamental significance in many other areas of science and technology.[20] Structure and dynamics of water in this region have been a subject of numerous theoretical investigations.[19,21] Some molecular dynamics simulations suggest that the self-diffusion of water in the interfacial region with 10:90% width of 3−4 Å is 50−100% higher than in the bulk water.[22−24] While some details of the water structure at the liquid−vapor interface such as an extent of hydrogen bonding and the orientation of the water dipole have been determined by vibrational sum frequency spectroscopy,[17,18] dynamic properties of water in this interfacial region have not been, thus far, experimentally accessible. We show here for the first time that 2-D voltammetric investigations of supercritical C_{14}TEMPO monolayers in the region of low surface densities open this possibility and hence the means to investigate the viscoelastic properties of this critical interface.

Experimental Section

Reagents. The synthesis of 4-tetradecaneamido-2,2,6,6-tetramethyl-1-piperidinyloxy (C_{14}TEMPO) involved a reaction of myristoyl chloride with 4-amino TEMPO in benzene according to a literature procedure.[25] Alternatively, myristoyl chloride was coupled to 4-amino-2,2,6,6-tetramethylpiperidine using the same

* Corresponding author. E-mail: majda@socrates.berkeley.edu.
[†] University of California at Berkeley.
[‡] University of Łódź.

10.1021/jp0031045 CCC: $20.00
Published on Web 12/16/2000

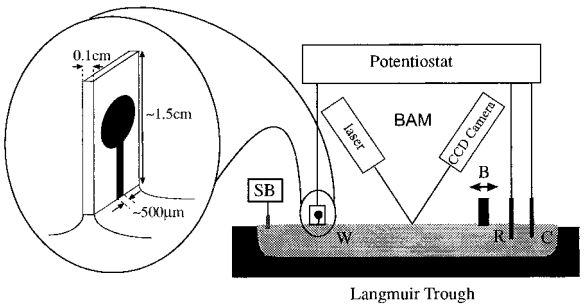

Figure 1. A schematic diagram of an experimental setup used to record $\pi-A$ isotherms, Brewster angle micrographs (BAM) and 2-D electrochemical data. **B**, movable barrier of the Langmuir trough; **C**, counter electrode; **R**, reference electrode; **W**, working line microelectrode; **SB**, surface film balance. The inset shows a line microelectrode as it touches the water surface.[27]

procedure and the resulting carboxamide was oxidized with hydrogen peroxide in the presence of sodium tungstate/EDTA catalyst in 1:6 acetone water solution according to a literature procedure.[26] Purification of the isolated product involved several column chromatography runs with alumina columns (with chloroform as eluting solvent) and florisil columns (using 1:1 methylene chloride, ethyl acetate solvent mixture). Elemental analysis was done and the melting point and pressure vs molecular area ($\pi-A$) isotherms were recorded following each chromatographic purification step until these results no longer changed following an additional run. The final results of elemental analysis were: calculated, C 72.4, H 11.9, N 7.3; found, C 72.48, H 11.78, N 7.22. The melting temperature was 52 °C. House-distilled H_2O was passed through a four-cartridge Millipore purification train, and a 0.2 μm hollow-fiber final filter. The resistivity of the resulting water (DI water) was >18.3 MW cm. Octadecyltrichlorosilane (OTS) and 3-mercaptopropyltrimethoxysilane (MPS) were from Aldrich. OTS was vacuum-distilled into sealed glass ampules, which were opened as needed immediately prior to the individual experiments. Octadecylmercaptan (OM) (Tokyo Kasei, Tokyo, Japan) was used without further purification. Reagent grade 70% $HClO_4$ (Fisher, ACS certified), chloroform (Fisher, ACS certified spectranalyzed), methanol (Fisher, spectroscopic grade), and all the other reagents were used as received.

Experiments on the Water Surface and Monolayer Techniques. A schematic diagram of the experimental set up is shown in Figure 1. Experiments at the air/water interface were carried out in a 10 × 20 cm^2 home-built Teflon trough equipped with a mechanically driven barrier (under computer control) and a Wilhelmy plate-type surface pressure microbalance. Filter paper was used to prepare Wilhelmy plates. Commercial, thermostated Langmuir trough instrument (KSV Model 2200) was used to record the $\pi-A$ isotherms. All experiments involving Langmuir troughs were done in an inert gas Plexiglass enclosure. The C_{14}TEMPO monolayers were spread from 1.0 mM chloroform solutions at 120 Å^2/molecule and compressed at 13 Å^2/molecule per minute. Brewster angle micrographs were recorded either with BAM2plus or BAM1 instruments (Nanofilm Technologie GmbH, Goettingen, Germany).

2-D Electrochemical Measurements. Electrochemical measurements at the air/water interface required specially designed "line" microelectrodes that can be positioned exactly in the plane of the air/water interface.[27] They were produced by creating a sharp gradient of wettability along a fracture line of ~800 Å thick gold films, vapor-deposited on microscope glass slides (ca. 8 × 20 mm^2). The pattern of the deposited gold film (see Figure 1) includes two circular areas, later used as electrical contact pads, and a strip of gold (0.5 mm in width) running between them. Prior to gold deposition, the glass substrates (Corning 2947) were treated with 3-mercaptopropyltrimethoxysilane (MPS) to induce adhesion of the vapor-deposited gold film. A modified MPS procedure relative to our original recipe[28] was used as follows. The glass slides were cleaned in a chromic acid solution for ~60 min. Following rinsing and drying, they were immersed in a 2% MPS solution in trichloroethylene (TCE) under nitrogen for 3−4 h. Subsequently, the slides were rinsed sequentially with TCE, acetone, 2-propanol, and DI water, and dried under a stream of nitrogen. They were then baked for ~10 min at 105−110 °C in a drying oven. Following gold vapor deposition, monolayers of octadecane mercaptan (OM) and octadecyltrichlorosilane (OTS) were formed on gold and on glass surfaces, respectively, by self-assembly to render all the surfaces of the substrate hydrophobic. By breaking such an electrode substrate in half (along a line drawn with a diamond pencil on the reverse side of the glass substrate perpendicular to the gold strip), one exposes a clean, and thus hydrophilic, edge surface of glass and gold, and creates two identical microelectrodes. These electrodes can then be positioned at the air/water interface by touching the water surface with the newly created edge surface. Thus, a line of wettability is formed along the edge of the gold micro-band between the hydrophilic gold cross sectional area and the hydrophobic (OM-coated) front face of the gold strip. The electrodes were always positioned at the air/water interface following monolayer spreading and solvent evaporation. Their performance at the air/water interface is typically reproducible for ~30 min. Later, contamination of the micro-band deteriorates the electrochemical signal and the electrode must be discarded. Cyclic voltammetry was done with an Ensman Model 852 bipotentiostat (Bloomington, IN) in a three-electrode configuration under computer control. The reference electrode (SCE or a quasi-reference, Ag wire) and a Pt counter electrode were immersed in the subphase in a Langmuir trough behind the barrier where their presence did not interfere with a monolayer compression.

Results and Discussion

The initial characterization of the C_{14}TEMPO monolayers involved surface pressure vs mean molecular area isotherms and Brewster angle microscopy. In Figure 2, we show the chemical structures and the $\pi-A$ isotherms for two electrochemically active amphiphiles of analogous structure, a long alkane chain ferroceneketone (C_{14}Fc) and C_{14}TEMPO. The structural similarities of these two amphiphiles involve identical chain lengths and similar, bulky, nonpolar fragments (ferrocene and TEMPO) located next to the primary polar groups of the two amphiphiles. The fact that the structure of the TEMPO amphiphile features the second polar group, the nitroxy radical moiety located across the otherwise lipophilic piperidine ring from the amide group is one perhaps significant structural difference. The two compounds exhibit identical limiting cross sectional areas, which can be obtained by extrapolating the steepest portions of the two isotherms to $\pi = 0$. The values are 53 ± 2 and 52 ± 2 Å^2/molecule, respectively. Clearly, the headgroups of these amphiphiles are substantially larger than the cross sectional areas of their alkane chains of ca. 20 Å^2/molecule.[1] Despite these structural similarities, the isotherms of these compounds exhibit significant differences. The most striking one concerns the shape of the $\pi-A$ isotherms in the low-pressure region. In the case of C_{14}Fc, surface pressure drops rapidly to zero at ~66 Å^2/molecule. A classical interpretation of $\pi-A$ isotherms suggests that at that point the C_{14}Fc monolayer undergoes a LE/G phase

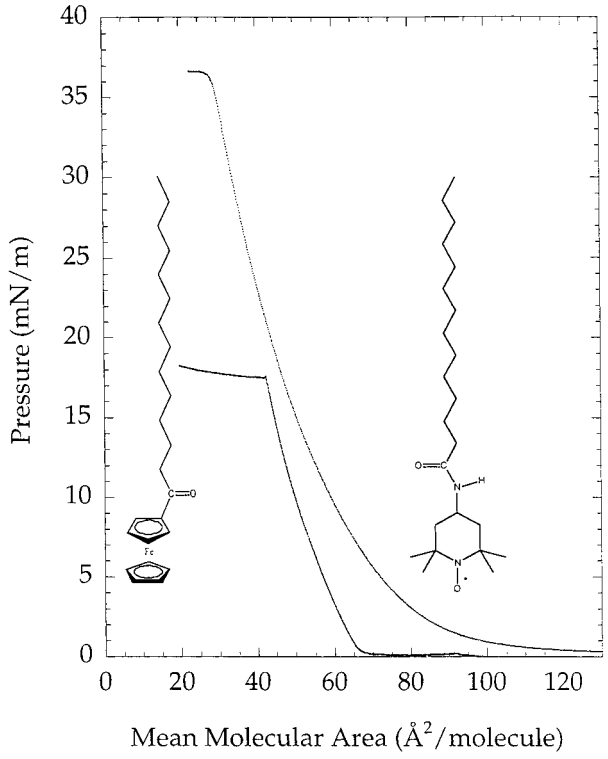

Figure 2. Pressure−area isotherms for C_{14}Fc (left) and C_{14}TEMPO (right) recorded on 50 mM $HClO_4$ and 50 mM HNO_3 subphases, respectively, at 22 °C.

transition. In contrast, a much more gradual pressure decrease is observed for C_{14}TEMPO with reproducibly measurable pressures (≥0.2 mN/m) persisting above 120 Å²/molecule. The C_{14}TEMPO monolayer can be expanded continuously without undergoing a phase transition. These data suggest that $T_c^{(l)}$ for C_{14}TEMPO is below room temperature.

The BAM images of the two monolayers concur with the conclusions drawn on the basis of the $\pi-A$ isotherms. Microscopic images of C_{14}Fc monolayers recorded at $A > 70$ Å²/molecule such as the one shown in Figure 3 clearly reveal a coexistence of circular 2-D gas "bubbles" with a liquid phase in this biphasic LE/G region. BAM images of C_{14}TEMPO monolayers are not shown since they are completely featureless at all surface densities, confirming the supercritical state of this system.

Even more convincing evidence of the supercritical state of the C_{14}TEMPO monolayer is provided by the 2-D voltammetric measurements. While TEMPO is a ubiquitous spin label, we take advantage here of its electroactivity. Reversible and kinetically facile properties of this cyclic nitroxide and its oxoammonium cation ($>N^{\bullet}-O - e \Leftrightarrow >N^{+}=O$) in both aprotic[29] and aqueous solutions [30] are well documented. In 2-D voltammetric experiments, we rely on the "line" microelectrodes positioned in the plane of the air/water interface (see Figure 1). These essentially one-dimensional electrodes are defined by a line of wettability that is created when a glass slide coated with a ~80 nm thick gold film (first rendered hydrophobic by self-assembly of an octadecanethiol monolayer) is fractured and placed on the water surface. The diffusion-controlled voltammograms obtained with the line electrodes can be interpreted in terms of the lateral diffusion constant of redox active amphiphiles on the water surface.[14,27,31] In addition, we discovered that the voltammetric signal can be relied on to diagnose

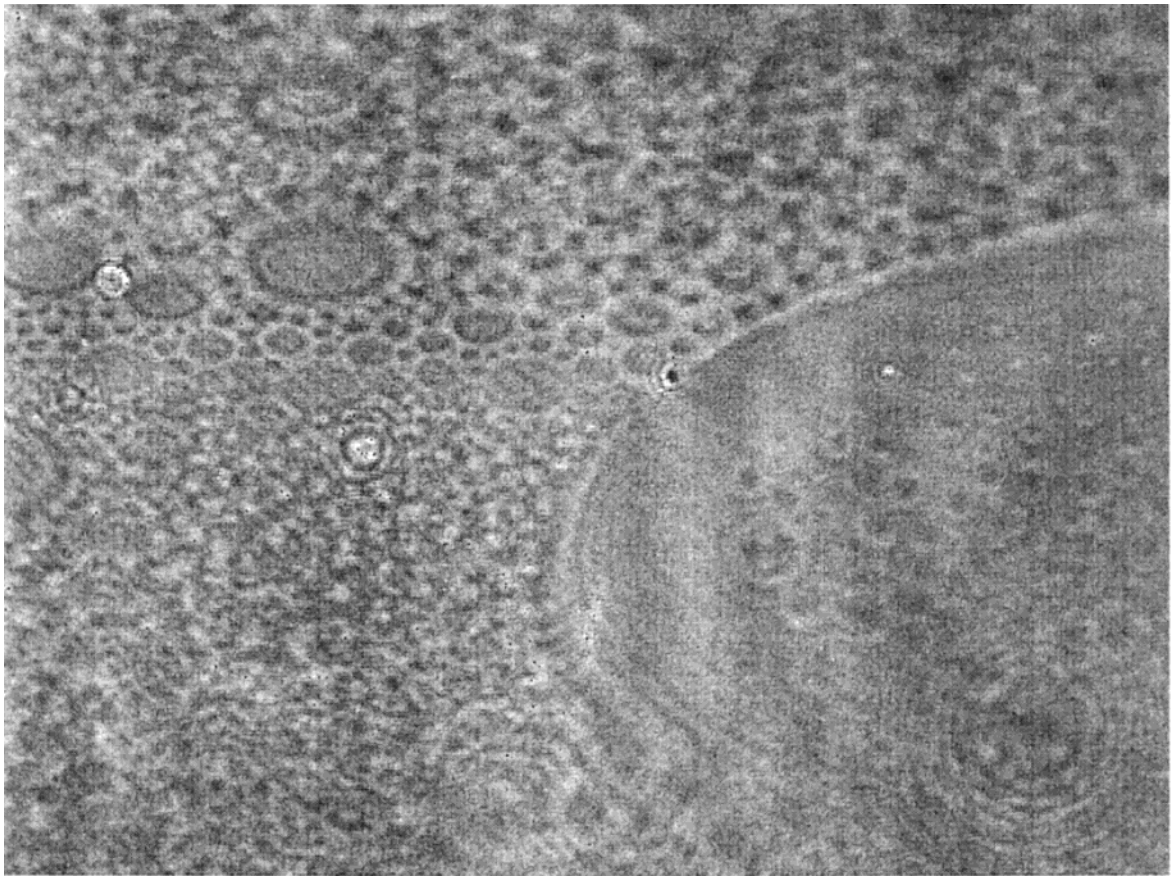

Figure 3. Brewster angle micrograph of C_{14}Fc monolayer obtained at 90 Å²/molecule in the LE/G coexistence region. The length of the shorter edge of the micrograph corresponds to 700 μm.

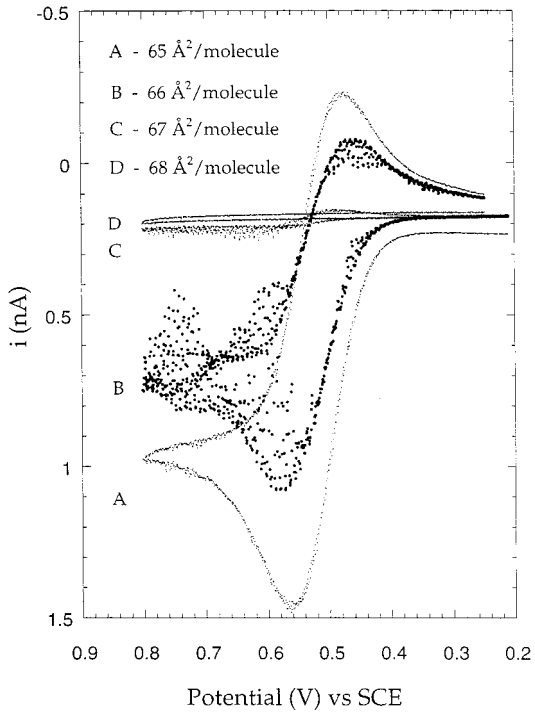

Figure 4. A set of four consecutive 2-D voltammograms recorded during a slow expansion of C_{14}Fc monolayer on 50 mM $HClO_4$ subphase. The mean molecular areas corresponding to each voltammogram are given in the figure. The $i-E$ curves were recorded with a 500 μm line microelectrode at 0.2 V/s. The disappearance of the voltammetric signal at 66−67 Å^2/molecule is due to the onset of the LE/G phase transition.

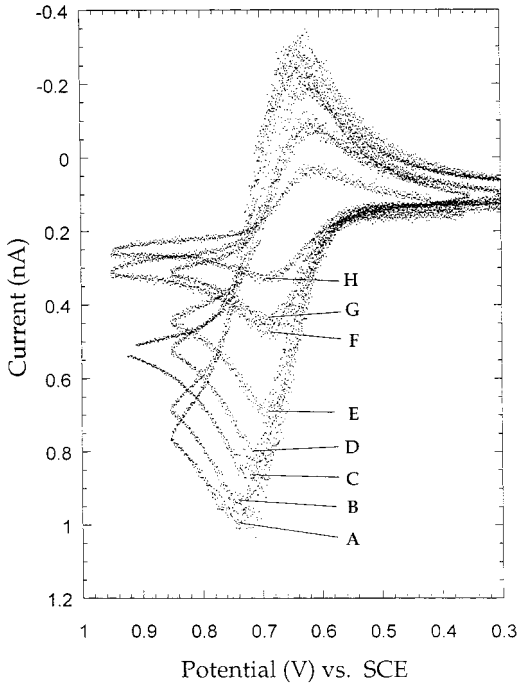

Figure 5. A collection of 2-D voltammograms of C_{14}TEMPO monolayer recorded with the 500 μm line microelectrodes at 0.2 V/s on 50 mM HNO_3 subphase. The mean molecular areas corresponding to each voltammogram are: A, 50; B, 70; C, 100; D, 120; E, 160; F, 320; G, 450; H, 600 Å^2/molecule.

the onset of a monolayer LE/G phase transition. Consider the set of 2-D voltammograms in Figure 4, recorded for a C_{14}Fc monolayer during its slow expansion. A well-developed $i-E$ curve recorded at 65 Å^2/molecule corresponds to the liquid region of this monolayer.[31] Upon expansion to 66 Å^2/molecule, a decrease of the voltammetric current as well as large current fluctuations are observed. This is followed by an abrupt disappearance of the signal at 67 Å^2/molecule. Clearly, the line microelectrode functions as a "boiling chip", nucleating formation of the C_{14}Fc gas phase. Since the surface concentration of the ferrocene amphiphile in the gas phase is likely to be at least an order of magnitude smaller than in the liquid phase, the voltammetric signal vanishes when the gaseous monolayer contacts the entire length (l) of the electrode. The sequence of the voltammograms in Figure 4 can be reproducibly reversed by recompression of the monolayer back to 65 Å^2/molecule. The onset of the LE/G phase transition determined this way takes place at 67 ± 2 Å^2/molecule, a value consistent with the one obtained from the $\pi-A$ isotherms. The supercritical state of the C_{14}TEMPO monolayer is reconfirmed by an analogous series of 2-D voltammograms in Figure 5. Clearly, no phase transition takes place upon expansion of this monolayer over a broad range of surface concentrations, resulting in a continuous series of voltammograms of slowly decreasing peak current (i_p). The latter reflects its dependence both on a decreasing surface concentration (Γ^*) and an increasing D:

$$i_p = 2.69 \times 10^5\, n^{2/3}\, l\, \Gamma^*\, D^{1/2}\, v^{1/2} \qquad (1)$$

where v is the scan rate (V s^{-1}).[27] The $\pi-A$ isotherms and 2-D voltammetry for C_{14}TEMPO were recorded at temperatures as low as 2 °C and yielded results identical to those reported in Figure 2. Thus the value of $T_c^{(I)}$ for C_{14}TEMPO could be substantially below room temperature. How the structure of C_{14}-TEMPO could account for its apparent supercritical behavior and how the structural elements of other TEMPO amphiphiles such as chain length and the polarity of the group that connects it to the piperidine ring determine the value of $Tc^{(I)}$ are subject of our current investigations.

A low $T_c^{(I)}$ value of the C_{14}TEMPO monolayers allows us to measure for the first time the dependence of the lateral diffusion constant of this amphiphile on its mean molecular area over a broad range of surface concentrations. The D values were deduced from the 2-D voltammograms such as those in Figure 5 using eq 1, and are plotted in Figure 6. The initially linear increase of D with A in the high surface density region for both C_{14}Fc and C_{14}TEMPO reflects an expected decreasing viscosity of the monolayer with expansion.[14,16,27,31] However, the plateau region observed for the C_{14}TEMPO system at A greater than ~250 Å^2/molecules has never been reported before for any Langmuir monolayer. In this low density region, the lateral diffusion of amphiphilic molecules is clearly no longer a subject of a drag in the hydrocarbon region. Instead, mobility of C_{14}-TEMPO is limited primarily by the viscous coupling to the subphase. The latter depends on the immersion depth of surfactant's headgroup and the viscoelastic properties of water near the vapor interface.

To interpret the lateral diffusion constant in the plateau region of Figure 6, we can rely on the Saffman and Delbrück hydrodynamic model[36] which we have used recently to interpret the lateral diffusion measurements of a series of ferroceneamide amphiphiles.[31] In this model, a probe amphiphile is treated as a cylinder with radius a located at the air/water interface as shown in Figure 7, where h_1 is the height of the hydrocarbon chain, and h_2 is the headgroup immersion depth. The cylinder diffuses laterally, experiencing viscous drag in both the hydrocarbon and headgroup regions, with effective viscosities η and

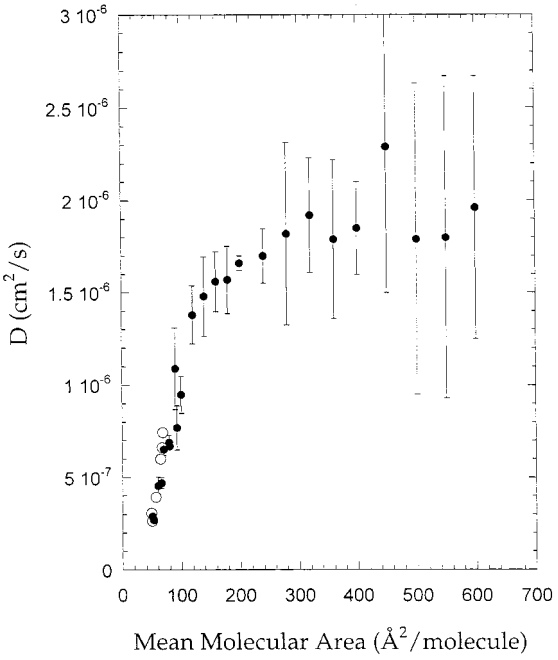

Figure 6. A plot of the lateral diffusion constant of C_{14}TEMPO on 0.050 M HNO_3 (closed circles) and of C_{14}Fc on 0.050 M $HClO_4$ subphase as a function of their mean molecular area. The *D* values were obtained from the 2-D voltammograms such as those in Figures 4 and 5. The large standard deviations (obtained with 12−16 independent measurements at each point) in the plateau region reflect expected, convectively induced density fluctuation in the C_{14}TEMPO monolayers. Their effect is magnified since *D* is proportional to i^2 (see eq 1).

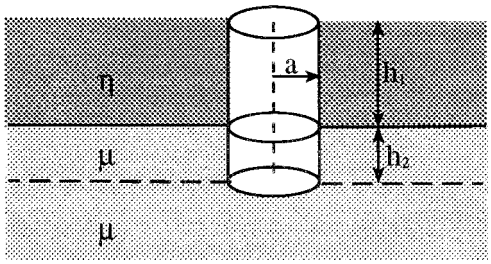

Figure 7. Hydrodynamic model of Saffman and Delbrück describing lateral diffusion of a cylindrical particle in a Langmuir monolayer of its own species at the air/water interface (see eq 3 and refs 31, 36). The darker gray area corresponds to monolayer's hydrocarbon region with average viscosity η. The lighter gray area represents the headgroup region in the aqueous subphase. The viscosity of this interfacial region (μ) can be different than that of the bulk water.

μ, respectively. Its diffusion constant is given by

$$D = \frac{kT}{4\pi(\eta h_1 + \mu h_2)}\left[\ln\frac{2}{\epsilon} - \gamma + \frac{4\epsilon}{\pi} - \left(\frac{\epsilon^2}{2}\right)\ln\frac{2}{\epsilon}\right] \quad (3)$$

where $\epsilon = \mu a/(\eta h_1 + \mu h_2)$, and γ is Euler's constant.[31] If we assume that the plateau region of Figure 6 is a true plateau, the product ηh_1 equals 0 according this model. As discussed below, this assumption may be a simplification. More precise diffusivity data are required to accurately determine the value of the slope in the "plateau" region in Figure 6. In either case, the viscosity of the interfacial region can be calculated from the measured *D* values if the immersion depth is measured or estimated from the molecular structure of the C_{14}TEMPO. Recent molecular dynamics simulations showed that the immersion depth of surfactants coincides with the size of their polar fragment.[19,37,38] To estimate *a*, it is reasonable to assume that in the plateau region the piperidinyloxy headgroup is oriented horizontally so that both of its polar fragments (amide and nitroxide) are hydrated. In view of this, *a* is 5−6 Å. Further, we estimate h_2 to be in a range of 4 to 6 Å. Adopting ηh_1 equals 0, a model of a cylindrical surfactant in Figure 7 is reduced to a disk with a 5−6 Å radius immersed in the subphase to a depth equal to its thickness of 4−6 Å. With these estimates of the geometric parameters, the *D* value in the plateau of 1.9×10^{-6} cm^2/s yields μ in the range 2.9−5.0 cP. Since the range of the immersion depth values adopted here is somewhat larger than the width of the water liquid−vapor interfacial region (10:90% width is ∼3.5 Å), we would perhaps expect to obtain a viscosity value similar to that of the bulk water, i.e., 1 cP. There are two reasons why μ is larger. The first is a small drag interaction expected to exist between the tetradecane chains and the water surface due to dispersion interactions.[19] The second relates to the relatively high density of the TEMPO groups in the water interfacial region. In other words, the viscoelastic properties of the interfacial region probed in our 2-D voltammetric experiments are those of a relatively concentrated, and thus more viscous, suspension of TEMPO groups in water, rather than those of pure water. The dependence of the viscosity (μ^*) of a suspension of solid particles on their concentration is a complex hydrodynamic problem, particularly for relatively concentrated suspensions.[39,40] In the limit of low concentrations, the problem has a solution in the form of Einstein's equation: $\mu^* = \mu(1 + 2.5\alpha)$, where μ is the viscosity of an ambient fluid and α is the concentration of particles by volume. It applies for $\alpha \leq 0.02$.[39,40] Clearly, our system exceeds the limits of applicability of that equation (at 600 $Å^2$/molecule, the lowest concentration of C_{14}-TEMPO for which *D* was measured in Figure 6, $\alpha = 0.15$). While more recent theories allow prediction of the viscosity of more concentrated suspensions,[40−42] we prefer to first expand our measurements to more dilute monolayer films and to measure the immersion depth of C_{14}TEMPO in the plateau region of Figure 6 using the procedure described previously.[31]

Conclusions

We presented experimental evidence based on the measurements of $\pi-A$ isotherms, BAM, and 2-D voltammetry demonstrating room-temperature supercritical fluid properties of C_{14}TEMPO Langmuir monolayers. We hypothesize that the unusually low critical temperature for the LE/G phase transition could be a result of a change of orientation of the TEMPO headgroup upon monolayer expansion. Experiments testing this hypothesis are in progress. The discovery of the room-temperature supercritical character of C_{14}TEMPO is significant in that it opens a possibility to use 2-D voltammetry to probe viscoelastic properties of the water liquid−vapor interfacial region. To this end, we have shown, for the first time, that the lateral mobility of an amphiphile becomes largely independent of its surface concentration when its mean molecular area is larger than ∼300 $Å^2$/molecule. Accurate measurements of the true viscosity of the aqueous interfacial region will require monolayers with densities as low as 2−5% monolayer coverage. Naturally, the measurements should involve a probe amphiphile exhibiting a shallow immersion depth so that it is comparable to the width of the water interfacial region. An amphiphilic TEMPO derivative in which >N•−O group is the only polar fragment is one such possibility. These requirements notwithstanding, the discovery of the room-temperature supercritical character of C_{14}TEMPO has removed one fundamental obstacle. It makes lateral mobility measurements possible far beyond 2-D liquid densities.

Acknowledgment. We express our gratitude to Professor Dietmar Möbius (MPI-Biophysical Chemistry, Göttingen) for offering us access to his BAM2plus instrument. We thank Professor Charles Knobler for illuminating discussions of phase behavior and critical phenomena in Langmuir monolayers. We also thank Rebecca Jockusch for the ab initio calculations of the structure of the TEMPO surfactant. This research was supported financially by the U.S. National Science Foundation under Grant CHE-0079225.

References and Notes

(1) Gaines, G. L. J. *Insoluble Monolayers at Liquid−Gas Interfaces*; Wiley-Interscience: New York, 1966.
(2) Cadenhead, D. A. Monomolecular Films as Biomembrane Models. In *Structure and Properties of Cell Membranes. Methodology and Properties of Membranes*; Benga, G., Ed.; CRC Press: Boca Raton, FL, 1985; Vol. 3, pp 21−62.
(3) Knobler, C. M.; Rashmi, C. D. *Annu. Rev. Phys. Chem.* **1992**, *43*, 207−236.
(4) Knobler, C. M. *Science* **1990**, *249*, 870−874.
(5) Möhwald, H. *Rep. Prog. Phys.* **1993**, *60*, 653−685.
(6) Möhwald, H. *Annu. Rev. Phys. Chem.* **1990**, *41*, 441−476.
(7) McConnell, H. M. *Annu. Rev. Phys. Chem.* **1991**, *42*, 171−195.
(8) Kaganer, V. M.; Möhwald, H.; Datta, P. *Rev. Mod. Phys.* **1999**, *71*, 779−819.
(9) Overbeck, G. A.; Möbius, D. *J. Phys. Chem.* **1993**, *97*, 7999−8004.
(10) Rivier, S.; Henon, S.; Meunier, J.; Schwartz, D. K.; Tsao, M.-W.; Knobler, C. M. *J. Chem. Phys.* **1994**, *101*, 10045−10051.
(11) Adam, N. K.; Jessop, G. *Proc. R. Soc. Ser. A* **1926**, *110*, 423−441.
(12) Moore, B. G.; Knobler, C. M.; Akamatsu, S.; Rondelez, F. A. *J. Phys. Chem.* **1990**, *94*, 4588−4595.
(13) Knobler, C. M. Recent Developments in the Study of Monolayers at the Air−Water Interface. In *Advances in Chemical Physics*; Progogine, I., Rice, S., Eds.; J. Wiley & Sons: New York, 1990; Vol. 77, pp 397−449.
(14) Majda, M. Translational Diffusion and Electron Hopping in Monolayers at the Air/Water Interface; In *Organic Thin Films and Surfaces*; Ulman, A., Ed.; Academic Press: San Diego, 1995; Vol. 20, pp 331−347.
(15) Peters, R.; Beck, K. *Proc. Natl. Acad. Sci. U.S.A.* **1983**, *80*, 7183−7187.
(16) Tamada, K.; Kim, S. H.; Yu, H. *Langmuir* **1993**, *9*, 1545−1550.
(17) Miranda, P. B.; Shen, Y. R. *J. Phys. Chem. B* **1999**, *103*, 3292−3307.
(18) Gragson, D. E.; Richmond, G. L. *J. Phys. Chem. B* **1998**, *102*, 3847−3861.
(19) Pohorille, A.; Wilson, M. A. *J. Mol. Struct. (THEOCHEM)* **1993**, *284*, 271−298.
(20) Lipowsky, R.; Sackmann, E. *Structure and Dynamics of Membranes*; Elsevier: Amsterdam, 1995; Vol. 1A and 1B.
(21) Benjamin, I. *Chem. Rev.* **1996**, *96*, 1449−1475.
(22) Townsend, R. M.; Rice, S. A. *J. Chem. Phys.* **1991**, *94*, 2207−2218.
(23) Benjamin, I. *J. Chem. Phys.* **1992**, *97*, 1432−1445.
(24) Taylor, R. S.; Dang, L. X.; Garrett, B. C. *J. Phys. Chem.* **1996**, *100*, 11720−11725.
(25) Rozantsev, E. G.; Suskina, W. I. *Akad. Nauk SSSR: Izvestiia; Ser. Khimicheskaia* **1969**, *5*, 1191−1193.
(26) Rozantsev, E. G.; Sholle, V. D. *Synthesis* **1971**, 190−202.
(27) Charych, D. H.; Landau, E. M.; Majda, M. *J. Am. Chem. Soc.* **1991**, *113*, 3340−3346.
(28) Goss, C. A.; Charych, D. H.; Majda, M. *Anal. Chem.* **1991**, *63*, 83−88.
(29) Krzyczmonik, P.; Scholl, H. *J. Electroanal. Chem.* **1992**, *335*, 233−251.
(30) Baur, J. E.; Wang, S.; Brandt, M. C. *Anal. Chem.* **1996**, *68*, 3815−3821.
(31) Kang, Y.-S.; Majda, M. *J. Phys. Chem. B* **2000**, *104*, 2082−2089.
(32) Schofield, K. R.; Rideal, E. K. *Proc. R. Soc. Ser. A* **1926**, *40*, 167−177.
(33) Fowkes, F. M. *J. Phys. Chem.* **1962**, *66*, 385−389.
(34) Gaines, G. L. *J. Phys. Chem.* **1978**, *69*, 924−930.
(35) Birdi, K. S. *Langmuir* **1991**, *7*, 3174−3175.
(36) Saffman, P. G.; Delbrück, M. *Proc. Natl. Acad. Sci. U.S.A.* **1975**, *72*, 3111−3113.
(37) Pohorille, A.; Benjamin, I. *J. Chem. Phys.* **1991**, *94*, 5599−5605.
(38) Pohorille, A.; Benjamin, I. *J. Phys. Chem.* **1993**, *97*, 2664−2670.
(39) Happel, J.; Brenner, H. *Low Reynolds Number Hydrodynamics with Special Applications to Particulate Media*; Prentice-Hall: Englewood Cliffs, NJ, 1965; Vol. Chapter 9, p 431−473.
(40) Lionberger, R. A.; Russel, W. B. Microscopic Theories of the Rheology of Stable Colloidal Dispersions. In *Advances in Chemical Physics*; Prigogine, I., Rice, S. A., Eds.; J. Wiley & Sons: New York, 2000; Vol. 110, pp 399−474.
(41) Cichocki, B.; Felderhof, B. U. *J. Chem. Phys.* **1988**, *89*, 3705−3709.
(42) Cichocki, B.; Felderhof, B. U. *J. Chem. Phys.* **1994**, *101*, 7850−7855.